# A density functional theory study on parameters fitting of ultra long armchair ($n$, $n$) single walled boron nitride nanotubes*

Wang Yan-Li(王艳丽)[a)†], Zhang Jun-Ping(张军平)[a)], Su Ke-He(苏克和)[a)], Wang Xin(王 欣)[a)], Liu Yan(刘 艳)[b)], and Sun Xu(孙 旭)[a)]

[a)] *Key Laboratory of Space Applied Physics and Chemistry, Ministry of Education of China, School of Natural and Applied Sciences, Northwestern Polytechnical University, Xi'an* 710072, *China*

[b)] *College of Chemistry and Life Science, Weinan Normal University, Weinan* 714000, *China*

(Received 11 October 2011; revised manuscript received 29 November 2011)

Armchair $(n, n)$ single walled boron nitride nanotubes with $n = 2$–17 are studied by the density functional theory at the B3LYP/3-21G(d) level combined with the periodic boundary conditions for simulating the ultra long model. The results show that the structure parameters and the formation energies bear a strong relationship to $n$. The fitted analytical equations are developed with correlation coefficients larger than 0.999. The energy gaps of $(2, 2)$ and $(3, 3)$ tubes are indirect gaps, and the larger tubes ($n = 4$–17) have direct energy gaps. Results show that the armchair boron nitride nanotubes ($n = 2$–17) are insulators with wide energy gaps of between 5.93 eV and 6.23 eV.

**Keywords:** boron nitride nanotubes, ultra long, periodic boundary conditions, formulas fitting

**PACS:** 03.65.–w, 78.67.–n, 81.07.De, 73.20.At **DOI:** 10.1088/1674-1056/21/6/060301

## 1. Introduction

Carbon nanotubes (CNTs), discovered by Iijima,[1,2] have received much attention in recent years due to their great physical and chemical properties. Boron nitride nanotubes (BNNTs) were theoretically predicted[3,4] in 1994 and successfully synthesized[5,6] in 1995. BNNT has a hexagon-like structure, which was similar to that of CNT. Research showed that the thermodynamic and chemical performance of single layered BN was much more stable than that of graphite.[7] Because of its outstanding mechanical properties, BNNT has a higher thermal conductivity, higher chemical stability, and better oxidation resistance than CNT.[7–13] Commonly, CNT has metal or semi-conductive characteristics, but BNNT showed insulation characteristics with a wide energy gap from 5.5 eV to 6 eV,[5,14,15] which was independent of diameter, chirality, and morphology.[16,17] Owing to the unique geometrical structure and uniform electrical behaviour,[18–20] BNNTs could be used in super-insulating protective shields of sensor and nano-electronics, in high strength insulating fibers in hazardous environments, or in hydrogen storage medium, sensor, catalyst carrier, and molecule-based logic gates.[21–24]

The Gaussian-type orbital (GTO) has been developed and transformed into a crystalline orbital with periodic boundary conditions (PBC) code by Bloch function,[25–27] which was first introduced into Gaussian-03 packages and employed in subsequent packages.[28] Now only a few theoretical studies on the ultra long nanotubes have been conducted using GTO-PBC model.[23] In our recent study, the ultra long armchair single walled $(n, n)$ CNTs ($n = 2$–20) were simulated, and the formation enthalpy and diameter of any $(n, n)$ CNT could be predicted.[29] Better fitted formula was desired which could show the change rules of formation enthalpies and the parameters of the ultra long model of BNNTs. Encouraged by our earlier work, in the present paper we investigate the single walled armchair $(n, n)$ BNNTs ($n = 2$–17) by the density functional theory (DFT) combined with the periodic boundary condition. The structure parameters and energies are examined and electronic properties are obtained.

*Project supported by the National Natural Science Foundation of China (Grant No. 50572089) and the Basic Research Foundation of Northwestern Polytechnical University (Grant No. JC201269).

†Corresponding author. E-mail: wangyanli@nwpu.edu.cn

© 2012 Chinese Physical Society and IOP Publishing Ltd

## 2. Calculation method and model

The Gaussian-09 packages[28] were used in the present work, and the density functional theory B3LYP combined with 3-21G(d) basis sets and the periodic boundary condition were employed. The one-dimensional (1D) PBC approach was used since it is sufficient for the nanotube model. All the geometries, energies, and the energy gaps were from the theoretical optimized structures.

For example, the optimized tube models (in which a primitive cell is shown as a solid atom) and the cross section structures of armchair $(5,5)$ and $(6,6)$ BNNT are shown in Fig. 1.

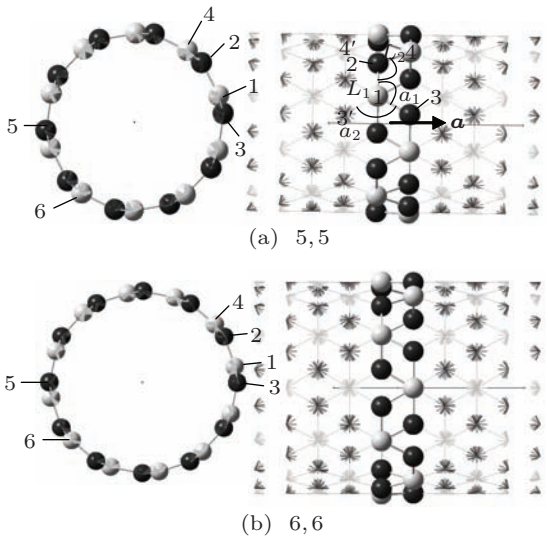



**Fig. 1.** Structures of single-walled boron nitride nanotubes: (a) $(5,5)$ tube and (b) $(6,6)$ tube, where N atoms are denoted as black balls and B atoms as white balls. The cross section structures and 1D tube model of each tube are shown. In the model the primitive cell of tube is shown as a solid atom.

It is found that there are two different kinds of chemical bonds: one has a perpendicular (circumferential) B–N bond length $L_1$ (the subscript 1 denotes the bond perpendicular to the tube axis) and the other has an oblique (axial) bond $L_2$ (the subscript 2 denotes the bond oblique with respect to the tube axis). For example, $L_1$ and $L_2$ represent the $B_1$–$N_2$ and the $B_1$–$N_3$ bond lengths denoted in Fig. 1, respectively. Similarly, the models contain two different kinds of bond angles: one is $\alpha_1$ that is the angle of a perpendicular bond combining with an oblique bond, and the other is $\alpha_2$ that is the angle consisting of two adjacent oblique bonds: one is $\alpha_1$ (NBN) and $\alpha_1$ (BNB) that are angles $N_2$–$B_1$–$N_3$ and $B_1$–$N_2$–$B_4$, the other is $\alpha_2$ (NBN) and $\alpha_2$ (BNB) that are angles $N_3$–$B_1$–$N_{3'}$ and $B_4$–$N_2$–$B_4$, which are denoted in Fig. 1.

CNT[29] has a smooth sidewall and contains a unique tube diameter, comparatively the sidewall of BNNT is not smooth, showing a wave structure. There exist two kinds of distances between two opposite atoms in the same cross section. The shorter distance is defined as the inner diameter ($D_1$) and the larger distance as the outside diameter ($D_2$). $D_1$ and $D_2$ pass through the centre of the cross section for the tubes with an even number $n$ but not for those of odd number $n$. For example, $D_1$ and $D_2$ are the distances of $B_1$-to-$N_5$ and $N_2$-to-$B_6$ for $(5,5)$ tube (Fig. 1(a)), and $D_1$ and $D_2$ are the distances of $B_4$-to-$B_6$ and $N_3$-to-$N_5$ for $(6,6)$ tube (Fig. 1(b)). $\boldsymbol{a}$ represents the translation vector of the primitive cell described in Fig. 1.

## 3. Results

### 3.1. Structure parameters

The relations between structure parameters and $n$ are shown in Fig. 2. The values of bond length ($L$), bond angle ($a$), tube diameter ($D$), the translation vector ($\boldsymbol{a}$), and the Mülliken atomic charges for B and N atoms are listed in Table 1.

As shown in Fig. 2(a), it is found that the perpendicular B–N bond length $L_1$ is always longer than the oblique bond length $L_2$. Both bond lengths of $L_1$ (BN) and $L_2$ (BN) decline with increasing $n$. The difference between $L_1$ (BN) and $L_2$ (BN) decreases with increasing $n$. $L_1$ and $L_2$ tend to their minimums of 0.1463 nm and 0.1462 nm when $n = 17$. The BNNT has an arched hexagon structure compared with the BN sheet, the difference between the bond lengths was due to the $\pi$-bond formed by a certain $sp^3$ hybrid along the tube axial direction. The perpendicular bond ($L_1$) is about 0.0037 nm longer and the oblique one ($L_2$) is about 0.0037 nm longer than the C–C bond length of pristine $(n,n)$ CNT[29] for $n \geq 4$. Their larger differences are found to be 0.012 nm ($L_1$) longer and 0.0022 nm ($L_2$) shorter for $n = 2$, and 0.022 nm ($L_1$) and 0.0029 nm ($L_2$) longer for $n = 3$.

For the convenience of estimating the parameters for other tubes, $L_1$ (BN) could be fitted to Eq. (1) or Eq. (2). The correlation coefficient ($R$) is 0.9992 or 0.9994, predicting that the fitting is accurate. $L_2$ (BN) could be fitted to Eq. (3) by least square method with $R = 0.9993$.

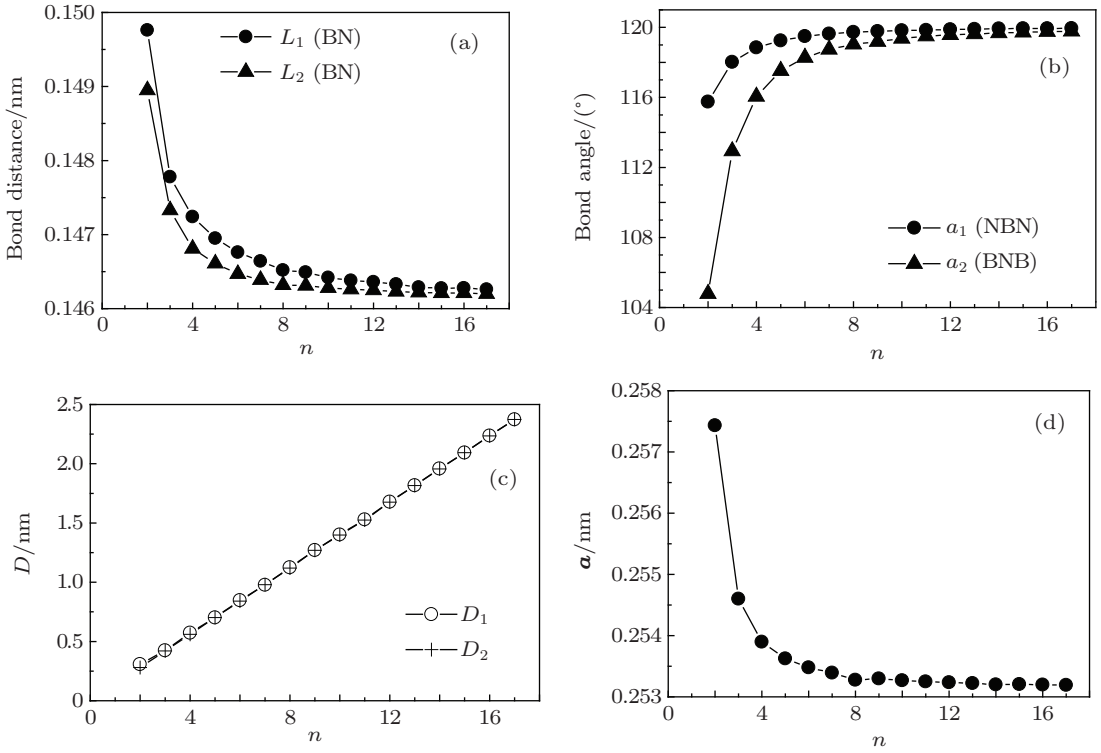



**Fig. 2.** Structure parameters of $(n, n)$ single-walled boron nitride nanotubes optimized by B3LYP/3-21G (d) method. Panel (a) shows the perpendicular bond ($L_{1,\mathrm{BN}}$) and the oblique bond ($L_{2,\mathrm{BN}}$) changing with $n$. Panel (b) exhibits the bond angles of $\alpha_{1,\mathrm{BNB}}$ and $\alpha_{1,\mathrm{NBN}}$ changing with $n$. Panel (c) indicates the inner diameter ($D_1$) and the outside diameter ($D_2$) changing with $n$. Panel (d) displays the translation vector $\boldsymbol{a}$ (for a primitive cell) changing with $n$.

$$L_1(\mathrm{BN}) = 0.003799/(n^1 + n^2 + n^3 + n^4 + n^5) + 0.14600 \text{ nm} \quad (2 \le n \le 32, R = 0.9992), \tag{1}$$

$$L_1(\mathrm{BN}) = 0.007830/n^{1.4} + 0.14611 \text{ nm} \quad (2 \le n \le 32, R = 0.9994), \tag{2}$$

$$L_2(\mathrm{BN}) = 0.011069/n^2 + 0.14616 \text{ nm} \quad (2 \le n \le 32, R = 0.9993). \tag{3}$$

As shown in Fig. 2(b), the curve of $\alpha_1$ (BNB) is below that of $\alpha_1$ (NBN). The values of $\alpha_1$ (BNB) and $\alpha_1$ (NBN) increase and their difference decreases with the increase of $n$. $\alpha_1$ (NBN) and $\alpha_1$ (BNB) tend to 119.95° and 119.78° respectively when $n = 17$. The bond angle is about 0.25° larger than the C–C–C bond angles of pristine $(n, n)$ CNT for $n \ge 4$. The larger differences were found to be 4.84° and 1.84° larger for $n = 2$ and $n = 3$, respectively.

$\alpha_1$ (NBN) and $\alpha_1$ (BNB) could be fitted to Eq. (4) with $R = 0.99996$ and Eq. (5) with $R = 0.9995$, respectively

$$\alpha_1(\mathrm{NBN}) = -61.0422/n^2 + 119.9764^\circ \quad (n \ge 2, R = 0.99996), \tag{4}$$

and

$$\alpha_1(\mathrm{BNB}) = -17.1391/n^2 + 119.9840^\circ \quad (n \ge 2, R = 0.9995). \tag{5}$$

In addition, $\alpha_2$ (NBN) and $\alpha_2$ (BNB), with angles 119.55° and 119.97°, are almost equal for $n \le 17$. They also increase with $n$ and tend to the value of 120°.

As shown in Fig. 2(c), $D_1$ and $D_2$ only have a little difference in a range from 0.0001 nm to 0.03 nm. The sidewall of CNT with nonpolar bond of C–C is uniform and smooth while that of BNNT is buckled tubular structure due to the polar bond of B–N. In practice, the difference between $D_1$ and $D_2$ decreases with increasing $n$. $D_1$ and $D_2$ are larger than the unique diameter ($D$) of CNT[29] with differences of about 0.035 nm or 0.040 nm for the same $n$ except that the inner diameter of $(2, 2)$ BNNT (0.2808 nm) is slightly smaller than that of CNT (0.2814 nm).

The fitted formula ($D_{\mathrm{CNT}} = 0.13530n + 0.01094$ nm, $n \ge 2$, $R = 0.99995$)[29]) for CNTs and the value of 0.2814 nm for $n = 2$ have been found in previous studies. $D_1$ and $D_2$ could be fitted to Eq. (6) and Eq. (7) with $R$ being 0.99998 and 0.99996, respec-

tively

$$D_1 = 0.13935n + 0.00392 \text{ nm} \quad (n \geq 2, R = 0.99998), \tag{6}$$

$$D_2 = 0.13859n + 0.01593 \text{ nm} \quad (n \geq 2, R = 0.99996). \tag{7}$$

The trend of translation vector $\boldsymbol{a}$ is described in Fig. 2(d). $\boldsymbol{a}$ decreases with the increase of $n$. The maximum of $\boldsymbol{a}$ was 0.25743 nm for $n = 2$ whereas the minimum of $\boldsymbol{a}$ was 0.25319 nm for $n = 17$. The translation vector $\boldsymbol{a}$ of BNNT is larger than that of CNT for the same $n$ except $n = 2$ ($\boldsymbol{a} = 0.26084$ nm for $(2, 2)$ CNT).[29] The $\boldsymbol{a}$ can be fitted to Eq. (8) with $R = 0.9992$

$$\boldsymbol{a} = 0.02947/n^{2.8} + 0.25322 \text{ nm} \quad (n \geq 2, R = 0.9992). \tag{8}$$

The Mülliken atomic charges for B and N atoms (denoted as Mülliken (B) and Mülliken (N)) are shown in Table 1. As expected, the Mülliken atomic charge of the B atom is always positive and that of the N atom is always negative due to the electronegativities of 2.04 and 3.04 (on the Pauling scale) for B and N atoms,[30] respectively. The conclusion can be drawn that the B atom is an electron donor whereas the N atom is an electron acceptor in a B–N atom pair. When $n$ varies from 2 to 17, the absolute values of Mülliken atomic charge for B and N atoms are equal for the same value of $n$, and increase from $0.811e$ to $0.953e$.

**Table 1.** Values of the following structure parameters of $(n, n)$ single-walled boron nitride nanotube at PBC-B3LYP/3-21G(d) level of theory: the perpendicular bond of $L_1$ (BN) and the oblique bond of $L_2$ (BN), bond angles of $\alpha_1$ (NBN), $\alpha_1$ (BNB), and $\alpha_2$ (NBN), the inner diameter ($D_1$), the outside diameter ($D_2$), and the translation vector ($\boldsymbol{a}$) of the primitive cell. Mülliken (B) and Mülliken (N) are the Mülliken atomic charges for B and N atoms, respectively.

| $n$ | $L_1$ (BN) /nm | $L_2$ (BN) /nm | $\alpha_1$ (BNB) /(°) | $\alpha_1$ (NBN) /(°) | $\alpha_2$ (NBN) /(°) | $D_1$ /nm | $D_2$ /nm | $\boldsymbol{a}$ /nm | Mülliken (B) /$e$ | Mülliken (N) /$e$ |
|---|---|---|---|---|---|---|---|---|---|---|
| 2 | 0.1498 | 0.1490 | 104.78 | 115.75 | 119.55 | 0.2808 | 0.3082 | 0.2574 | 0.811 | –0.811 |
| 3 | 0.1478 | 0.1473 | 112.94 | 118.02 | 119.57 | 0.4210 | 0.4243 | 0.2546 | 0.878 | –0.878 |
| 4 | 0.1472 | 0.1468 | 116.05 | 118.84 | 119.68 | 0.5611 | 0.5728 | 0.2539 | 0.899 | –0.899 |
| 5 | 0.1470 | 0.1466 | 117.52 | 119.24 | 119.78 | 0.7017 | 0.7021 | 0.2536 | 0.913 | –0.913 |
| 6 | 0.1468 | 0.1465 | 118.27 | 119.49 | 119.83 | 0.8406 | 0.8476 | 0.2535 | 0.923 | –0.923 |
| 7 | 0.1466 | 0.1464 | 118.74 | 119.63 | 119.87 | 0.9794 | 0.9778 | 0.2534 | 0.931 | –0.931 |
| 8 | 0.1465 | 0.1463 | 119.03 | 119.73 | 119.88 | 1.1191 | 1.1244 | 0.2533 | 0.936 | –0.936 |
| 9 | 0.1465 | 0.1463 | 119.18 | 119.78 | 119.91 | 1.2689 | 1.2702 | 0.2533 | 0.941 | –0.941 |
| 10 | 0.1464 | 0.1463 | 119.37 | 119.82 | 119.92 | 1.3984 | 1.4028 | 0.2533 | 0.943 | –0.943 |
| 11 | 0.1464 | 0.1463 | 119.50 | 119.84 | 119.93 | 1.5243 | 1.5307 | 0.2532 | 0.945 | –0.945 |
| 12 | 0.1464 | 0.1462 | 119.57 | 119.88 | 119.94 | 1.6755 | 1.6784 | 0.2532 | 0.947 | –0.947 |
| 13 | 0.1463 | 0.1462 | 119.62 | 119.90 | 119.95 | 1.8160 | 1.8168 | 0.2532 | 0.950 | –0.950 |
| 14 | 0.1463 | 0.1462 | 119.68 | 119.92 | 119.96 | 1.9555 | 1.9588 | 0.2532 | 0.950 | –0.950 |
| 15 | 0.1463 | 0.1462 | 119.72 | 119.93 | 119.96 | 2.0940 | 2.0941 | 0.2532 | 0.952 | –0.952 |
| 16 | 0.1463 | 0.1462 | 119.75 | 119.94 | 119.97 | 2.2344 | 2.2371 | 0.2532 | 0.952 | –0.952 |
| 17 | 0.1463 | 0.1462 | 119.78 | 119.95 | 119.97 | 2.3731 | 2.3742 | 0.2532 | 0.953 | –0.953 |

The optimized structures are distorted for a thin tube of $n \leq 4$, which are shown in Fig. 3. The cross section structure of a $(2, 2)$ tube is a parallelogram formed from four atoms as shown in Fig. 3(a). The length and the width (i.e., the length of perpendicular bond) are 0.2536 nm and 0.1498 nm respectively. As a result, the sidewall of the (2,2) BN–NT is an obviously serrated structure as reported.[31–33] The length of diagonal exactly equal to the outside diameter of tube ($D_2 = 0.3082$ nm) is in good agreement with the experiment data (0.3 nm) of the thinnest single walled CNT[34] (regarded as $(2, 2)$ tube in theoretical calculation). The cross sections of $(3, 3)$ and $(4, 4)$ tubes look like a hexagon and an octagon as shown in Figs. 3(b) and 3(c), respectively. Results show that the curvature may not be ignored for a small tube. The tubes resemble cylinders for the large tubes ($n \geq 5$).

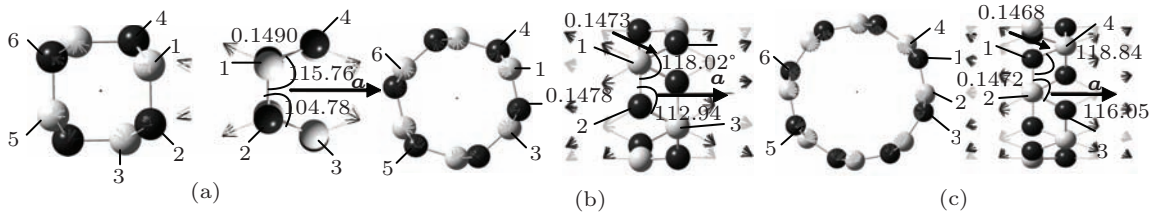



**Fig. 3.** Cross sections and primitive cell structures of $(n, n)$ single-walled boron nitride nanotubes for little tube optimized by B3LYP/3-21G(d) method (bond length: nm, bond angle: °). N atoms are denoted as black balls and B atoms as white balls. Panel (a) is for a $(2, 2)$ tube, panel (b) for a $(3, 3)$ tube, and panel (c) for a $(4, 4)$ tube.

## 3.2. Energy

The optimized energy of a primitive cell containing $2n$ B–N pairs for $(n, n)$ BN–NTs is denoted as $E_n$. The energy for 1-mol B or N atom is defined as $\Delta E_n$ $[\Delta E_n = (E_n/2n)]$. $\Delta E_n$ decreases with the increase of $n$ as shown in Fig. 4(a). $\Delta E_n$ has the high values of $-79.247962$ a.u. $(n = 2)$ and $-79.278532$ a.u. $(n = 3)$. For $n = 7$–17, the values are between $-79.301288$ a.u. and $-79.304647$ a.u. with a little difference of 0.003359 a.u. $\Delta E_n$ can be fitted to Eq. (9) with the correlation coefficient $R = 0.9995$ for $n \geq 2$

$$\Delta E_n = 0.23104/n^2 - 79.30501 \text{ a.u. with } R = 0.9995 \text{ for } n \geq 2. \quad (9)$$

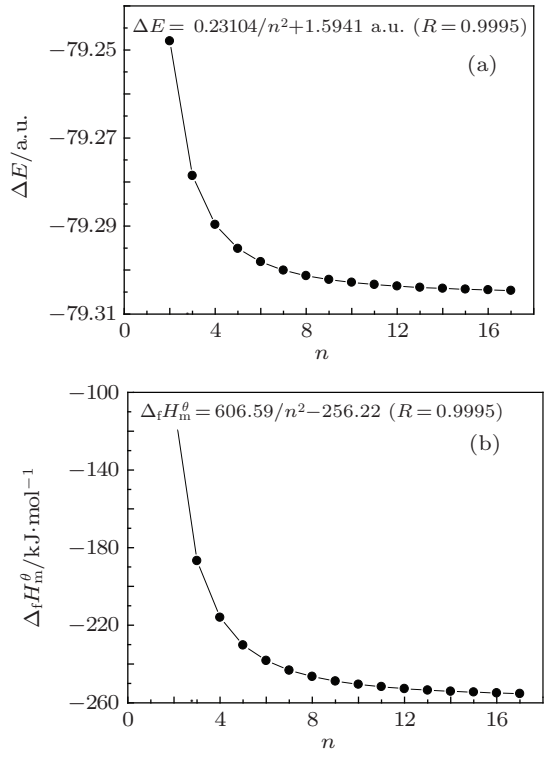



**Fig. 4.** Relationships between (a) $\Delta E_n$ and $n$ and between (b) $\Delta_f H_m^\theta$ and $n$.

The formation enthalpy $(\Delta_f H_m^\theta)$ of BN–NT obtained using atomic reaction method is exhibited in Fig. 4(b). $\Delta_f H_m^\theta$ is calculated from Eq. (10) (the correlation coefficient $R = 0.9995$). The values of $\Delta_f H_m^\theta$ are $-106.45$ kJ·mol$^{-1}$ $(n = 2)$ and $-186.71$ kJ·mol$^{-1}$ $(n = 3)$. Similar to $\Delta E_n$, the values of $\Delta_f H_m^\theta$ are between $-250.47$ kJ·mol$^{-1}$ and $-255.27$ kJ·mol$^{-1}$ with a little difference of 3.8 kJ·mol$^{-1}$ when $n = 11$–17

$$\Delta_f H_m^\theta = 606.58894/n^2 - 256.22593 \text{ kJ} \cdot \text{mol}^{-1} \quad (n \geq 2, R = 0.9995). \quad (10)$$

In previous investigation,[29] the formation enthalpy of $(n, n)$ SWCNT was predicted to follow a formula $[\Delta_f H_m^\theta = 409.47/n^2 + 8.63$ kJ·mol$^{-1}$ $(R = 0.9997, n \geq 2)]$. It is found that the enthalpy of BN–NT with a negative value is far lower than that of CNT. It could be inferred that BN–NT is more stable than CNT. The difference between corresponding values is 215 kJ·mol$^{-1}$ $(n = 2)$. The difference tends to an invariable value of about 263 kJ·mol$^{-1}$ $(n \geq 12)$.

## 3.3. Energy gap

The energy gap $(E_g)$ is the difference in energy between the lowest unoccupied crystal orbital $(E_{LUCO})$ and the highest occupied crystals orbital $(E_{HOCO})$. These values vary with $n$ as shown in Figs. 5(a) and 5(b). Compared with band structure of pristine $(n, n)$ CNT, where the energy gaps show metal $(n \geq 3)$ and semiconductor properties $(n = 2, 3)$.[29] Results show that the armchair boron nitride nanotubes $(n = 2$–17) are insulators with a wide energy gap. The values of $E_g$ are 5.930 eV $(n = 2)$ and 6.064 eV $(n = 3)$ and between 6.194eV and 6.235 eV $(4 \leq n \leq 17)$. Clearly, The results are close to the previous theoretical and experimental values[5,14,15] with a slight difference of 0.2 eV–0.3 eV. The value of $E_{HOCO}$ is between $-6.684$ eV and $-6.426$ eV, and the value of $E_{LUCO}$ is between $-0.754$ eV and $-0.192$ eV.

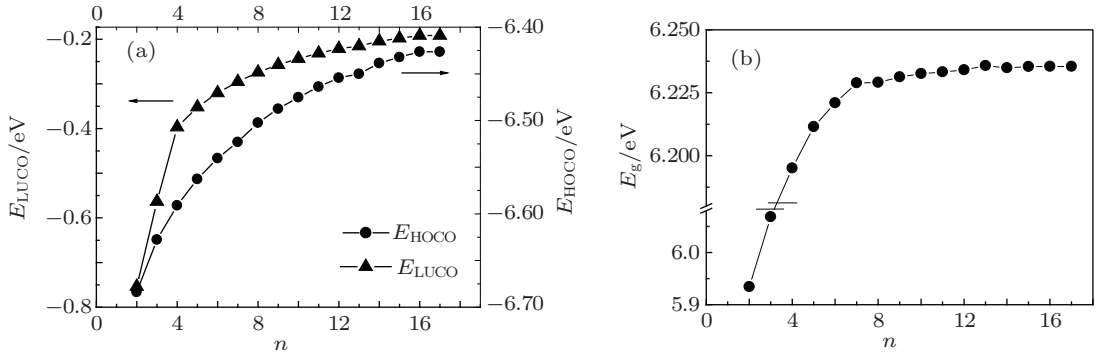



**Fig. 5.** Curves of $E_{\rm HOCO}$, $E_{\rm LUCO}$ versus $n$ (a) and $E_{\rm g}$ versus $n$ (b) of $(n, n)$ boron nitride nanotubes optimized by B3LYP/3-21G(d) method.

Some band structure examples are shown in Fig. 6 where the five highest occupied (solid curves) and the five lowest unoccupied (dashed curves) bands are plotted. The $\boldsymbol{k}$ point of wave vector $\boldsymbol{k}$ is default in the present work. $\Gamma$ point is the centre of the first Brillouin zone and the distance of $\Gamma$ point to $X$ point is half the width of the Brillouin zone. However, all the bands exhibit some degree of quasi-degeneration. It is interesting that $(2, 2)$ and $(3, 3)$ boron nitride nanotubes have indirect gaps (i.e., the maximum of the valence band and the minimum of the empty band are not at the same $\boldsymbol{k}$ point). It is clearly shown that the models for $n$ being 5, 10 or 17 each have a direct band gap (i.e., the maximum of the valence band and the minimum of the empty band are at the same $\boldsymbol{k}$ point).

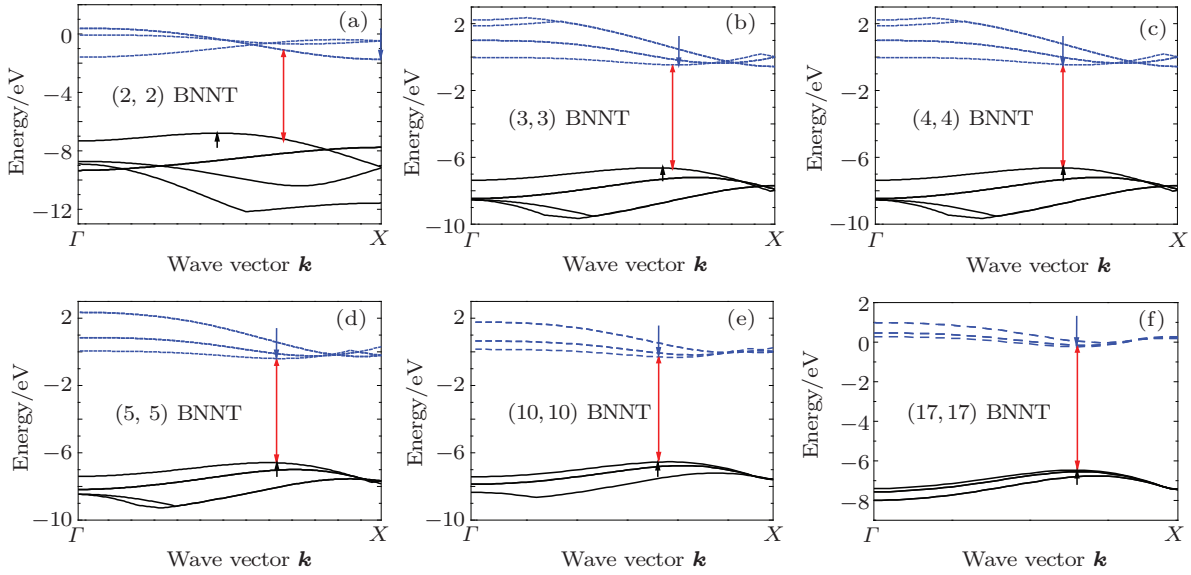



**Fig. 6.** (colour online) Band structures of the most stable BNNT nanotubes optimized with PBC-B3LYP/3-21G(d) method. The solid curves are for the five highest occupied bands and the dashed ones for the five lowest unoccupied bands. The location indicated by an arrow is the minimum of the LUCO or the maximum of the HOCO band. Panel (a) is for the band structure of $(2, 2)$ BNNT tube, panel (b) for the band structure of $(3, 3)$ BNNT tube, panel (c) for the band structure of $(4, 4)$ BNNT tube, panel (d) for the band structure of $(5, 5)$ BNNT tube, panel (e) for the band structure of $(10, 10)$ BNNT tube, and panel (f) for the band structure of $(17, 17)$ BNNT tube.

## 4. Conclusion

The ultra long armchair $(n, n)$ single-walled boron nitride nanotubes ($n$ = 2–17) are studied using the density functional theory combined with the periodic boundary conditions. The structure parameters, energies and energy gaps are examined with B3LYP/3-21G(d) method.

It is found that the perpendicular bond is always longer than the oblique bond (axial B–N bond). The bond angle (included between a parallel bond and an oblique bond) of NBN is always larger than that of BNB. The structure parameters and $n$ are strongly related. For the convenience of estimating the parameters of $(n, n)$ single-walled boron nitride nanotubes for any tube, the bond length and bond angle can be well fitted with $R > 0.9992$. The energy and the formation enthalpy can be predicted with a correlation coefficient of 0.9995.

The energy gaps of $(2, 2)$ and $(3, 3)$ tubes are both indirect gaps, and the larger tubes ($n = 4$–17) are all direct energy gaps. Results show that the armchair boron nitride nanotubes ($n = 2$–17) are insulators with wide energy gaps between 5.93 eV and 6.23 eV.

## Acknowledgement

Part of the calculations were performed in the High Performance Computation Center of the Northwestern Polytechnical University.

## References

[1] Iijima S 1991 *Nature* **354** 56
[2] Iijima S 1993 *Mater. Sci. Eng.* B **19** 172
[3] Rubio A, Corkill J L and Cohen M L 1994 *Phys. Rev.* B **49** 5081
[4] Blase X, Rubio A, Louie S G and Cohen M L 1994 *Europhys. Lett.* **28** 335
[5] Chopra N G, Luyken R J, Cherrey K, Crespi V H, Cohen M L, Louie S G and Zettle A 1995 *Science* **269** 966
[6] Loiseau A, Willaime F, Demoncy N, Hug G and Pascard H 1996 *Phys. Rev. Lett.* **76** 4737
[7] Pouch J J and Alterovitz A 1990 *Synthesis and Properties of Boron Nitride* (Zürich: Trans. Tech. Publications) p. 54
[8] Maryam M and Mahmoud M 2010 *Physica* E **42** 2147
[9] Gorbunova M A, Shein I R, Makurin Y N, Ivanovskaya V V, Kijko V S and Ivanovskii A L 2008 *Physica* E **41** 164
[10] Loiseau A, Willaime F, Demoncy N, Schramchenko N, Hug G, Colliex C and Pascard H 1998 *Carbon* **36** 743
[11] Golberg D, Bando Y, Tang C C and Zhi C Y 2007 *Adv. Mater.* **19** 2413
[12] Han W Q, Zett L A and Am J 2002 *Chem. Soc.* **125** 2062
[13] Sueyavanshia A P, Yu M F, Wen J G, Tang C C and Yoshio B 2004 *Appl. Phys. Lett.* **84** 2527
[14] Chopra N G and Zettle A 1998 *Sol. St. Comm.* **105** 297
[15] Chen Y, Zou J, Campbell S J and Gerard L C 2004 *Appl. Phys. Lett.* **84** 2430
[16] Wu J, Han W Q, Walukiewicz W, Ager J W, Shan W, Haller E E and Zettl A 2004 *Nano Lett.* **4** 647
[17] Vaccarini L, Goze C, Henrard L, Hernández E, Bernier P and Rubio A 2000 *Carbon* **38** 1681
[18] Takeo O, Naruhiro K and Katsuaki S 2008 *Diamond Relat. Mater.* **17** 1805
[19] Takeo O, Naruhiro K and Katsuaki S 2008 *Phys. Chem. Solid* **69** 1228
[20] Moradian R and Azadi S 2006 *Physica* E **35** 157
[21] Zhi C Y, Bando Y, Tang C C and Golberg D 2010 *Mater. Sci. Eng.* (R: Reports) **70** 92.
[22] Villalpando-Paez F, Zamudio A, Elias A L, Son H, Barros E B, Chou S G, Kim Y A, Muramatsu H, Hayashi T, Kong J, Terrones H, Dresselhaus G, Endo M, Terrones M and Dresselhaus M S 2006 *Chem. Phys. Lett.* **424** 345
[23] Chou Y M, Wang H W, Lin Y J, Chen W H and Wang B C 2009 *Diamond Relat. Mater.* **18** 351
[24] Takeo O and Ichihito N 2002 *Physica* B: *Conden. Matter* **323** 216
[25] Feibelman P J 1987 *Phys. Rev.* B **35** 2626
[26] Jaffe J E and Hess A C 1996 *Chem. Phys.* **105** 10983
[27] Dovesi R, Civalleri B, Orlando R, Roetti C, Saunders V R, Lipkowitz K B, Larter R and Cundari T R (eds.) 2005 *Reviews in Computational Chemistry* (New York: Wiley) **21** pp. 1–11
[28] Frisch M J, Trucks G W, Schlegel H B, Scuseria G E, Robb M A, Cheeseman J R, Scalmani G, Barone V, Mennucci B, PeterssonA P, Nakatsuji H, Caricato M, Li X, Hratchian H P, Izmaylov A F, Bloino J, Zheng G, Sonnenberg J L, Hada M, Ehara M, Toyota K G, Fukuda R, Hasegawa J, Ishida M, Nakajima T, Honda Y, Kitao O, Nakai H, Vreven T, Montgomery J A, Peralta J E, Ogliaro F, Bearpark M, Heyd J J, Brothers E, Kudin K N, Staroverov V N, Kobayashi R, Normand J, Raghavachari K, Rendell A, Burant J C, Iyengar S S, Tomasi J, Cossi M, Rega N, Millam J M, Klene M, Knox J E, Cross J B, Bakken V, Adamo C, Jaramillo J, Gomperts R, Stratmann R E, Yazyev O, Austin A J, Cammi R, Pomelli C, Ochterski J W, Martin R L, Morokuma K, Zakrzewski V G, Voth G A, Salvador P, Dannenberg J J, Dapprich S, Daniels A D, Farkas O, Foresman J B, Ortiz J V, Cioslowski J and Fox D J 2009 *Gaussian* 09, Revision A.02, Gaussian, Inc., Wallingford CT
[29] Wang Y L, Su K H, Wang X and Liu Y 2011 *Acta Phys. Sin.* **60** 098111 (in Chinese)
[30] Truhlar D G, Isaacson A D and Garrett B C 1985 *The Theory of Chemical Reaction Dynamics* (Boca Raton: CRC Press) p. 65
[31] Blase X, Vita A D, Charlier J and Car R 1998 *Phys. Rev. Lett.* **80** 1666
[32] Srivastava D, Menon M and Cho K 2001 *Phys. Rev.* B **63** 195413
[33] Menon M and Srivastava D 1999 *Chem. Phys. Lett.* **307** 407
[34] Zhao X, Liu Y, Inoue S, Suzuki T, Jones R O and Ando Y 2004 *Phys. Rev. Lett.* **92** 125502